
Calculated Scission-Neutron Properties in Unexpected Agreement with Data on Prompt Neutrons

N. Carjan^{1,2}, M. Rizea²,

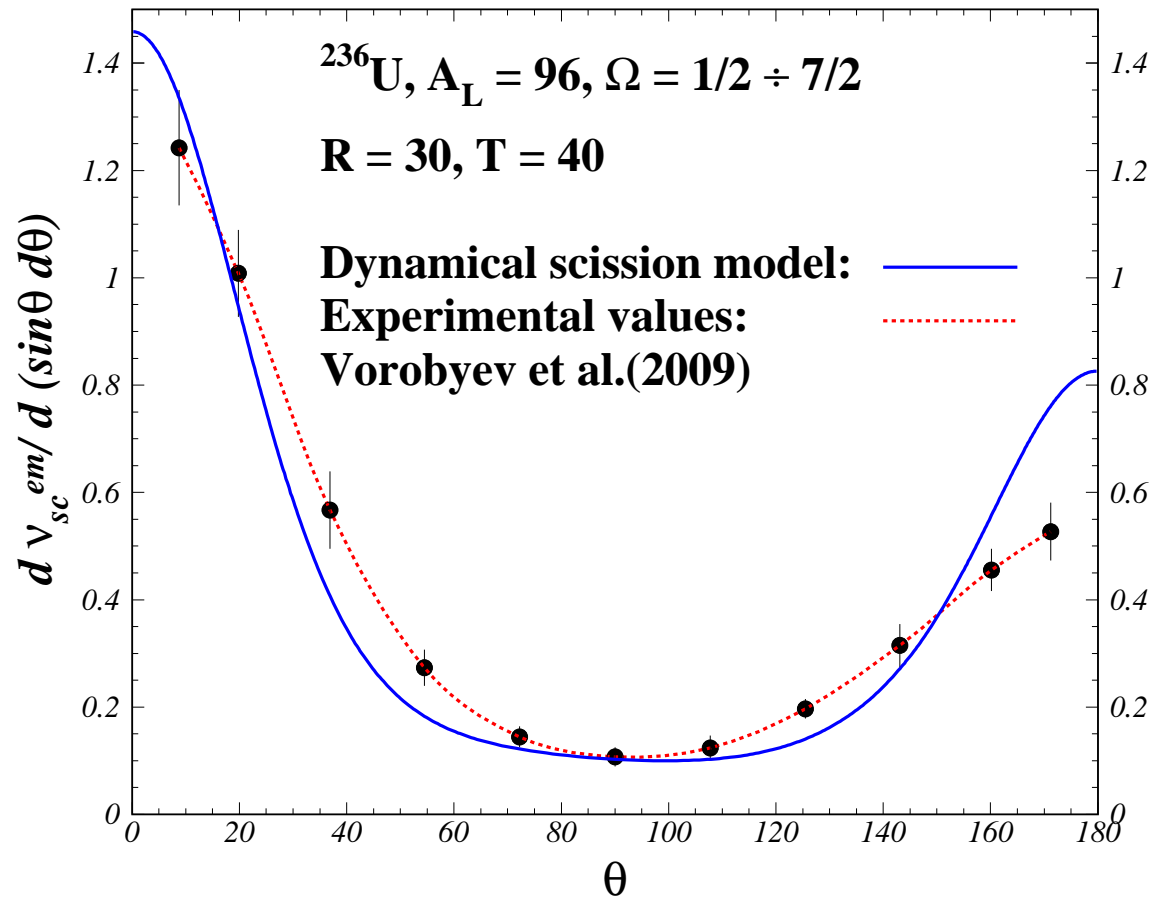
(1) CENBG, CNRS/IN2P3 - Université Bordeaux 1, France

**(2) "Horia Hulubei" National Institute of Physics and
Nuclear Engineering, Bucharest, Romania**

Plan

- Title explained on the:
 - 1) Angular distribution with respect to the fission axis and related quantity $\rightarrow \nu_L/\nu_H$
 - 2) Distribution of kinetic energies
 - 3) Average multiplicity
- Dynamical Scission Model (Formalism):
 - 1) Excitation energy and neutron multiplicity
 - 2) Probability and current densities
- Selected numerical results:
 - 1) Time dependent decay rate
 - 2) What influences the angular distribution?
 - 3) "Saw-tooth" structures.

Calculated and experimental angular distribution; $\Delta\theta = 16^\circ$



Note the resemblance of the data with our calculations (except the widths on both sides).

Scission neutron multiplicity: L vs H fragment

\mathbf{A}_L	70		96		118	
	ν_{sc}	ν_L/ν_H	ν_{sc}	ν_L/ν_H	ν_{sc}	ν_L/ν_H
$\mathbf{T}/10^{-22}$						
1	0.667	0.891	0.561	1.075	0.612	1.
\mathbf{T}	ν_{sc}^{em}	ν_L/ν_H	ν_{sc}^{em}	ν_L/ν_H	ν_{sc}^{em}	ν_L/ν_H
10	0.109	1.759	0.118	1.424	0.121	1.
20	0.247	1.056	0.258	1.348	0.283	1.
30	0.315	1.077	0.363	1.402	0.346	1.
40	0.352	1.066	0.429	1.414	0.377	1.

The ratio corresponds to two regions of the interval (0, 180), the separation point being obtained in terms of the neck position. They represent neutrons which move left and right with respect to a plane perpendicular to the neck.

Scission neutron multiplicity: L vs H fragment

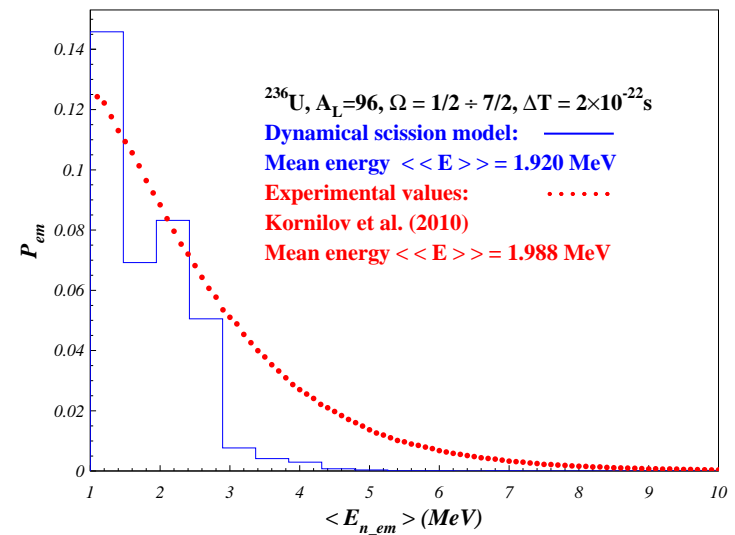
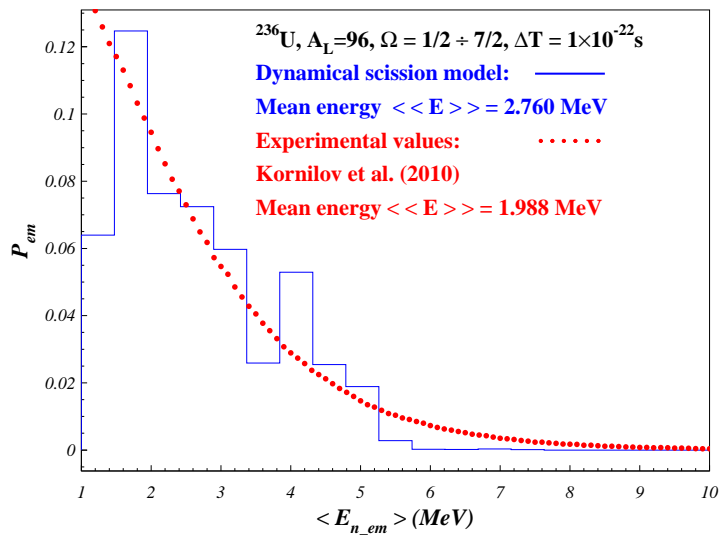
\mathbf{T}	\mathbf{A}_L		70		96		118	
	ν_{sc}^{em}	ν_L/ν_H	ν_{sc}^{em}	ν_L/ν_H	ν_{sc}^{em}	ν_L/ν_H		
10	0.109	1.901	0.118	1.448	0.121	1.		
20	0.247	1.218	0.258	1.378	0.283	1.		
30	0.315	1.282	0.363	1.469	0.346	1.		
40	0.352	1.288	0.429	1.540	0.377	1.		

The ratio corresponds to the regions: $\theta \in [0, 50]$ and $\theta \in [130, 180]$. All the states corresponding to $\Omega = 1/2, \dots, 7/2$ have been taken into account.

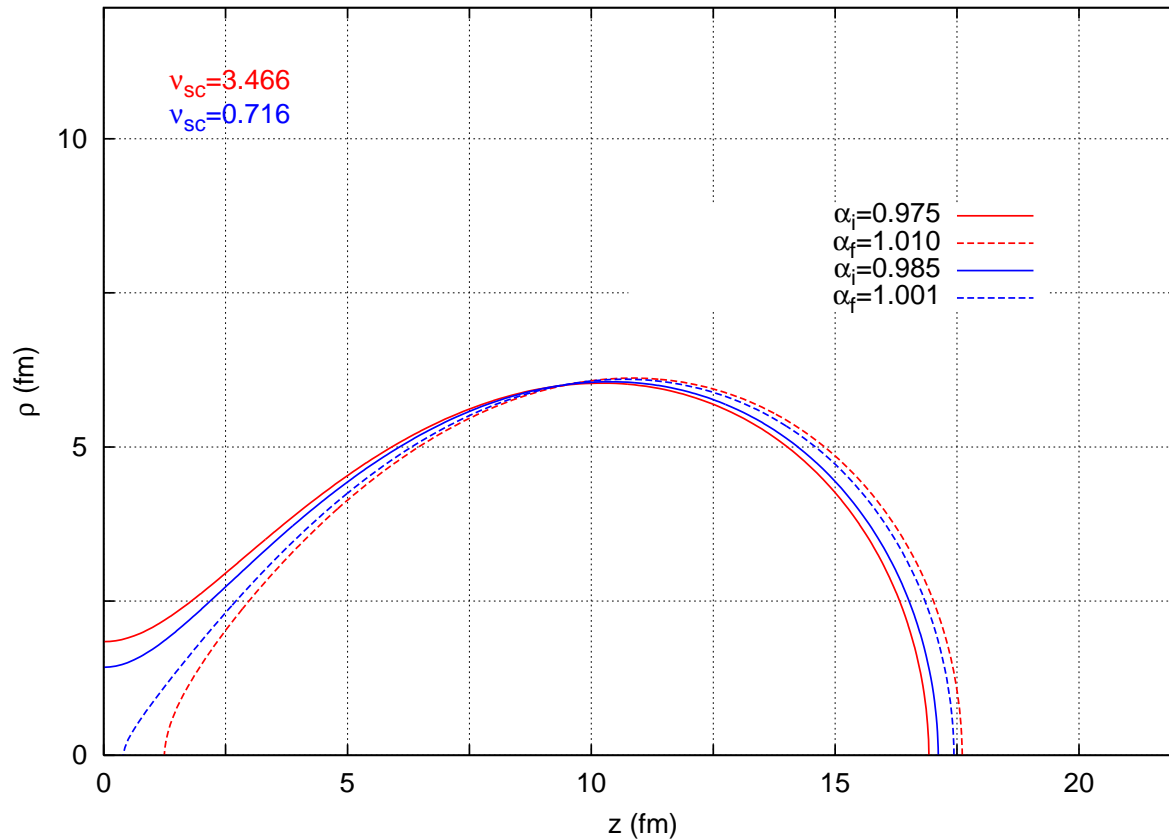
Histogram of the average scission-neutron energy

immediately after scission ($\alpha=1.001$) for two transition times ΔT

The experimental prompt-neutron spectrum is also shown to compare the trends: the slope and the range.

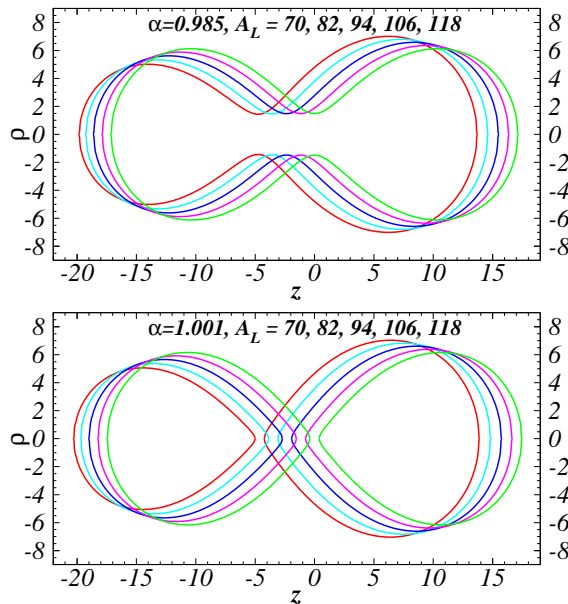


Length of scission jump and neutron multiplicity



Increasing r_{neck}^{min} from 1.6 to 1.9 fm quadruples ν_{sc}
N. Carjan, P. Talou, O. Serot, NuclPhysA792(2007)102

Modeling a diabatic transition at scission (neck rupture)



Equipotential lines $V_0/2$ (just-before and immediately-after scission) for different mass asymmetries.

A fast transition at scission produces the excitation of all neutrons that are present in the surface region. There is a small probability that this excitation exceeds the binding energy leading to neutron release.

This process is easy to study in the sudden approximation ($\Delta T=0$):
N.Carjan, M.Rizea,
Phys.Rev.C82(2010)014617

Going beyond the sudden approximation

A time-dependent approach to the fast transition at scission:

$\{\alpha^i\} \rightarrow \{\alpha^f\}$: M.Rizea, N.Carjan,
Nucl.Phys.A909(2013)50.

Features of this **scission model**:

- 1) **dynamical**: it takes into account the finite duration ΔT of the neck rupture and its integration in the fragments
- 2) **microscopic**: it calculates the time evolution of each occupied single-neutron state (shell model)
- 3) **fully quantum mechanical**: it uses the two-dimensional time-dependent Schrödinger equation (TDSE2D) with time-dependent potential (TDP).

Most previous models were statical (statistical, semiclassical or constrained Hartree-Fock).

The picture behind the present model was first proposed by Fuller (Wheeler) in 1962 and illustrated by a "volcano erupting" in the middle of a Fermi sea.

Dynamical scission model: formalism

It is a generalization of the sudden approximation. Let $|\Psi^i\rangle$, $|\Psi^f\rangle$ be the eigenfunctions corresponding to the just-before-scission and immediately-after-scission configurations respectively. The propagated wave functions $|\Psi^i(t)\rangle$ are wave packets that have also some positive-energy components. The probability amplitude that a neutron occupying the state $|\Psi^i\rangle$ before scission populates a state $|\Psi^f\rangle$ after scission is

$$a_{if} = \langle \Psi^i(T) | \Psi^f \rangle = 2\pi \int \int (g_1^i(T)g_1^f + g_2^i(T)g_2^f) d\rho dz.$$

The result strongly depends on the duration T of the scission process.

Excitation energy of the fission fragments

The total occupation probability of a given final eigenstate is:

$$V_f^2 = \sum_{bound} v_i^2 |a_{if}|^2$$

where v_i^2 is the ground-state occupation probability of a given initial eigenstate. Since V_f^2 is different from v_f^2 (the ground-state value), the fragments are left in an excited state. The corresponding **excitation energy at scission** is:

$$E_{sc}^* = 2 \sum_{bound\ states} (V_f^2 - v_f^2) e_f.$$

The factor of 2 is due to the spin degeneracy.

Neutrons emitted at scission

One can also calculate the multiplicity of the neutrons released during scission:

$$\nu_{sc} = 2 \sum_{bound} v_i^2 \left(\sum_{unbound} |a_{if}|^2 \right).$$

A quantity that can clarify the emission mechanism of the scission neutrons is the probability density i.e., the spatial distribution of the emission points at $t=T$

$$S_{em}(\rho, z) = 2 * \sum_{bound} v_i^2 |\Psi_{em}^i(\rho, z, T)|^2,$$

where

$$|\Psi_{em}^i\rangle = |\Psi^i(T)\rangle - \sum_{\text{bound states}} a_{if} |\Psi^f\rangle$$

is the part of the wave packet that is emitted.
Similarly, the current density

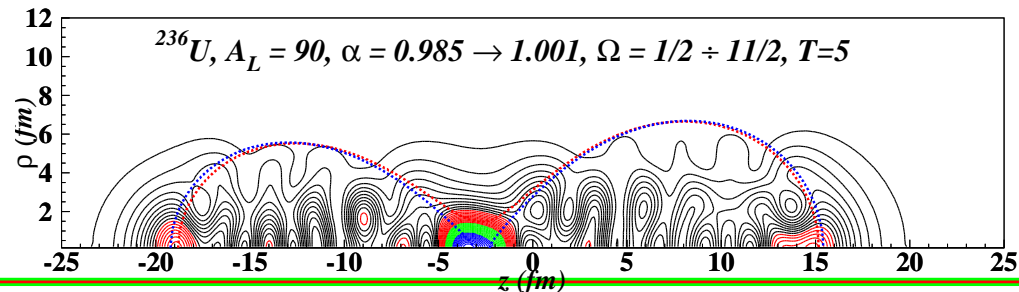
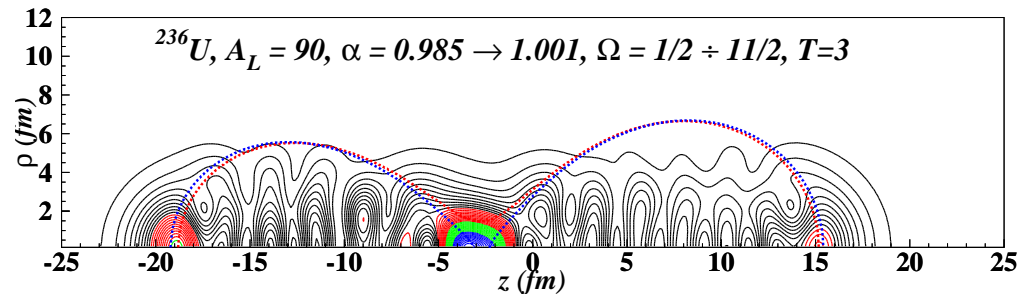
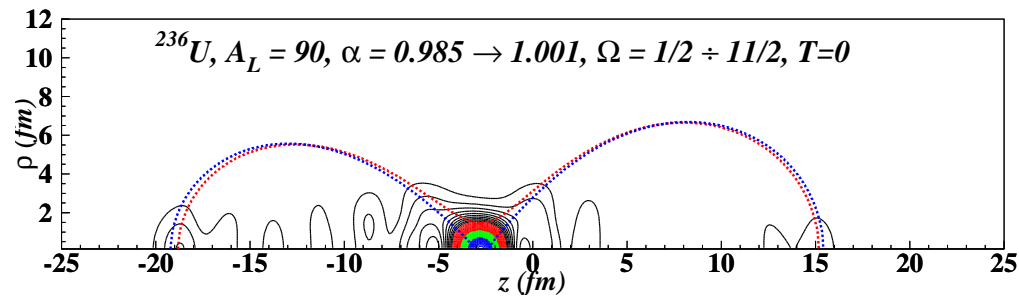
$$\bar{D}_{em}(\rho, z) = \frac{i\hbar}{\mu} \sum_i v_i^2 (f^i \bar{\nabla} f^{i*} - f^{i*} \bar{\nabla} f^i), \quad (1)$$

with $f^i = |\Psi_{em}^i\rangle$, provides **the distribution of the average directions of motion** of the unbound neutrons at $t=T$.

These two quantities influence the amount of neutrons that are reabsorbed, scattered or left unaffected by the fragments and finally determine their angular distribution.

Emission points ($A_L=90$; all Ω ; $\Delta T=0,3,5 \times 10^{-22}$ sec)

with increasing ΔT the emission points migrate from the H to the L fragment and from the inter-fragment to the inside-fragment regions



Partition among the fission fragments (1)

Finally it is interesting to separate the contributions of the light (L) and of the heavy (H) fragment using the probability of each emitted (or excited) neutron to be present in the L (or H) fragment:

$$E_{sc}^*(L, H) = \sum_f e_f (V_f^2 - v_f^2) N_f^{L,H}$$

$$\nu_{sc}(L, H) = \sum_i v_i^2 \left(\sum_f |a_{if}|^2 \right) N_i^{L,H},$$

where the partial norms $N_{i,f}^{L,H}$ are given by:

Partition among the fission fragments (2)

$$N_{i,f}^L = 2\pi \int_0^R \int_{-Z}^{z_{min}} \left[\left(g_1^{i,f} \right)^2 + \left(g_2^{i,f} \right)^2 \right] d\rho dz$$

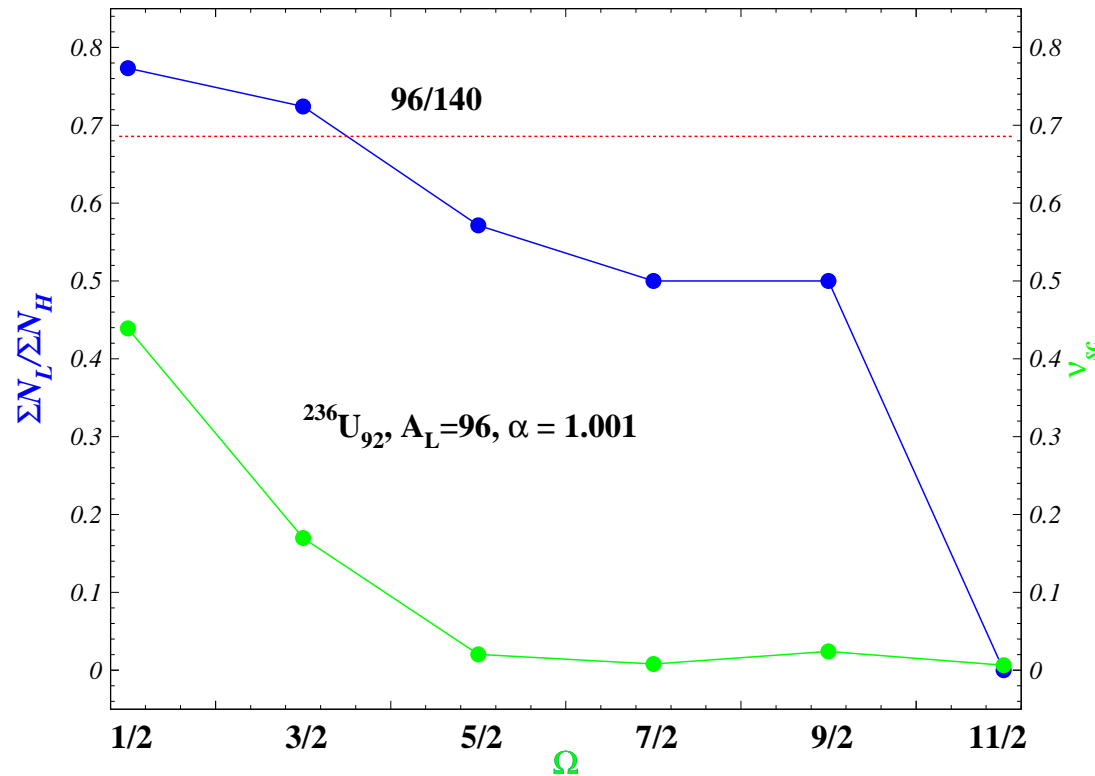
$$N_{i,f}^H = 2\pi \int_0^R \int_{z_{min}}^Z \left[\left(g_1^{i,f} \right)^2 + \left(g_2^{i,f} \right)^2 \right] d\rho dz$$

z_{min} corresponds to the neck position, identified as the point between $-Z$ and Z where an equipotential line has a minimum.

The knowledge of $E_{sc}^*(L,H)$ is important since it enters into the Monte-Carlo Hauser-Feschbach simulation of the neutron evaporation from the accelerated fragments.

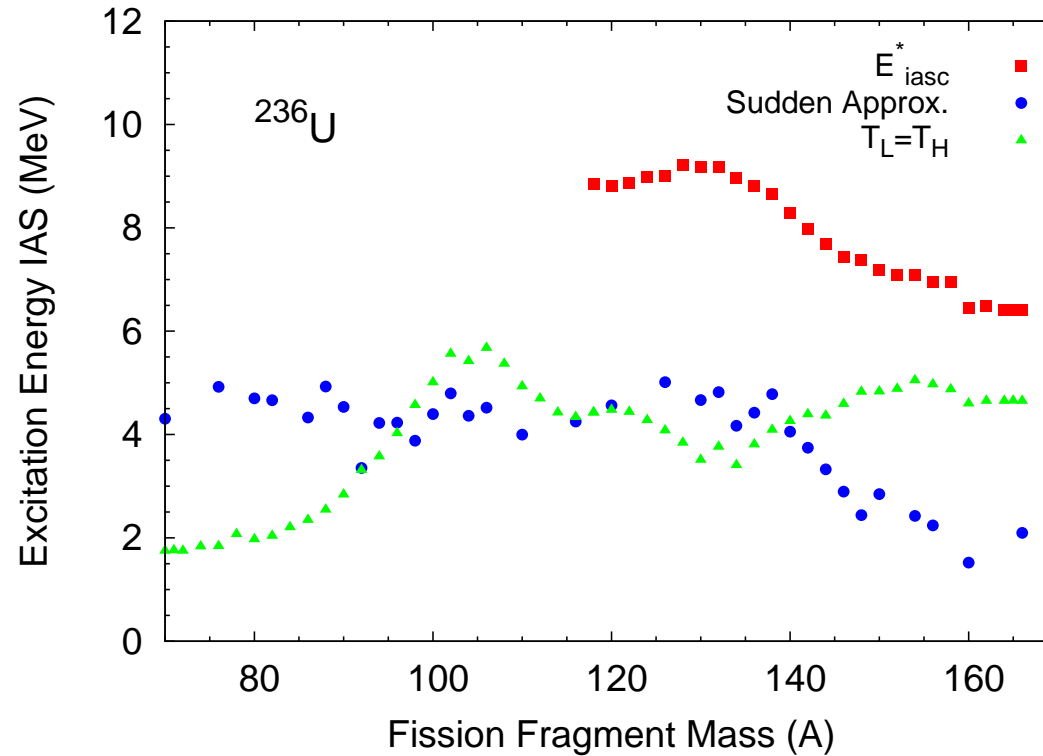
Distribution of neutrons with given Ω between L and H

Explains why the light fragment emits more neutrons.



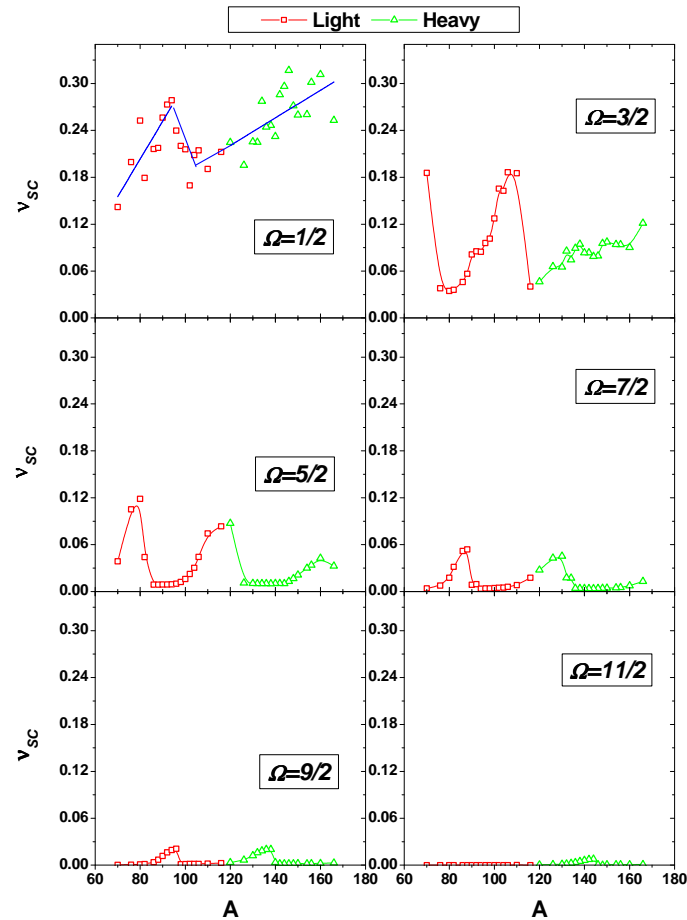
It is a trivial property of the Nilsson orbitals in asymmetric double-well potentials. Nothing to do with more deformation or temperature.

Partition laws



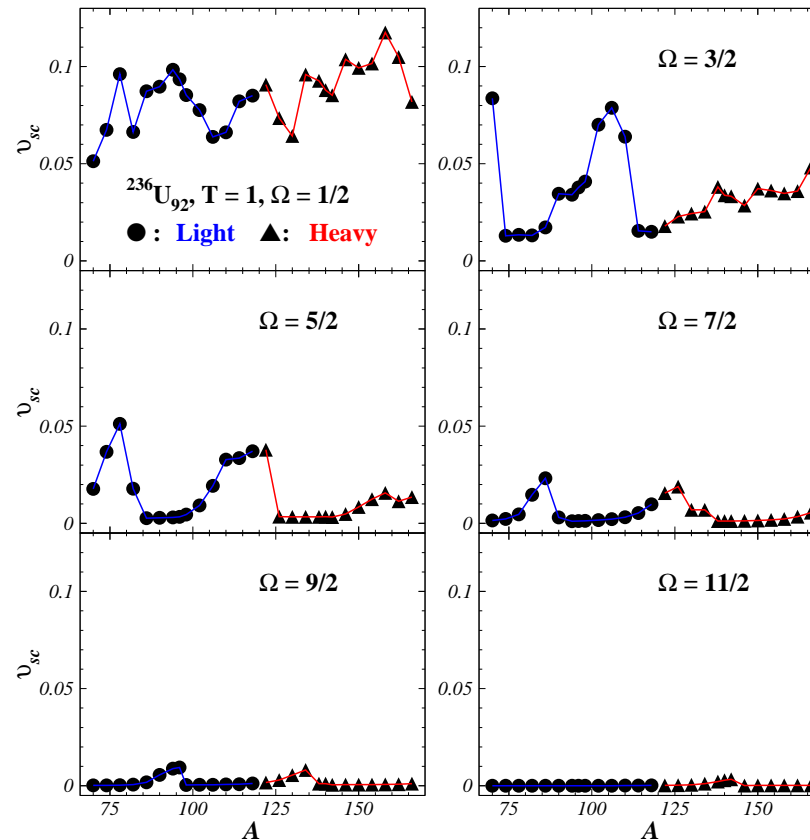
thermalization vs sudden approximation

Neutron multiplicity function of fission-fragment mass



the 'saw-tooth' is a nuclear structure effect

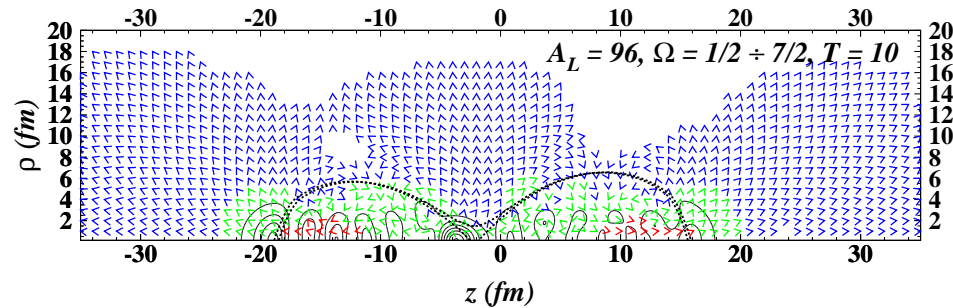
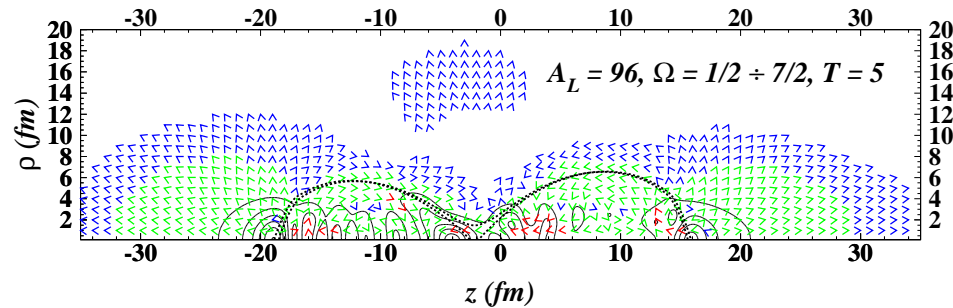
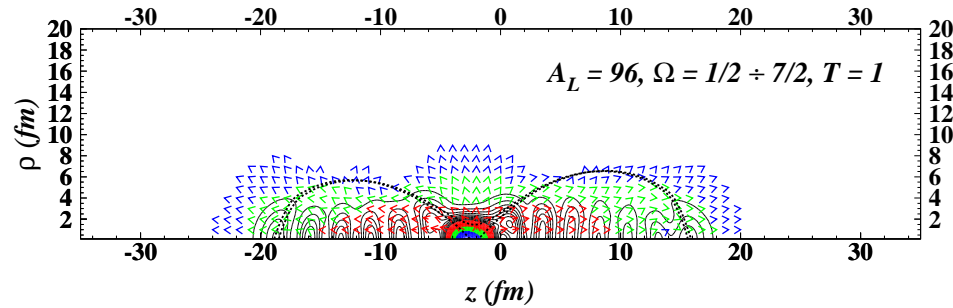
$\nu_{sc}(A)$ for each Ω at $\Delta T=1$



the time-dependence preserves the 'saw-tooth' structure

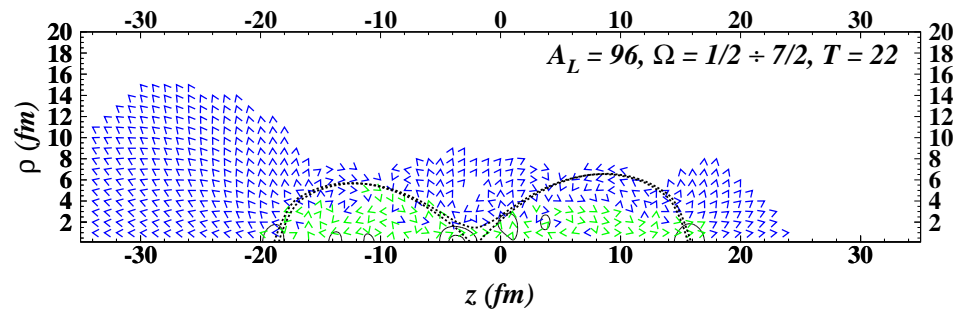
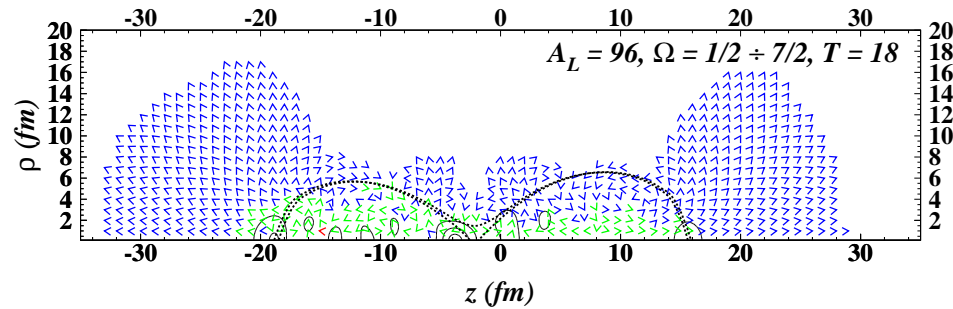
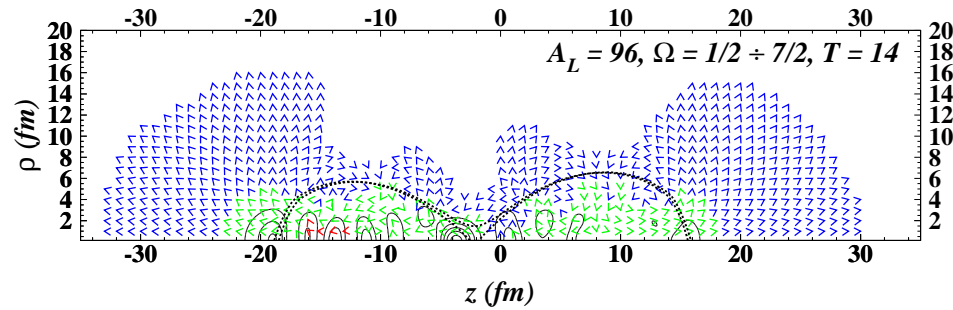
Emission directions ($A_L=96$; all Ω ; $T=1,5,10 \times 10^{-22}$ sec)

correlation between S_{em} and D_{em} ; pulsed emission perpendicular



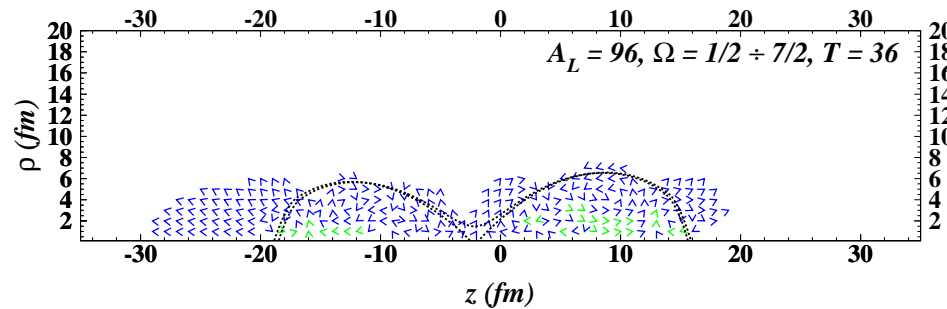
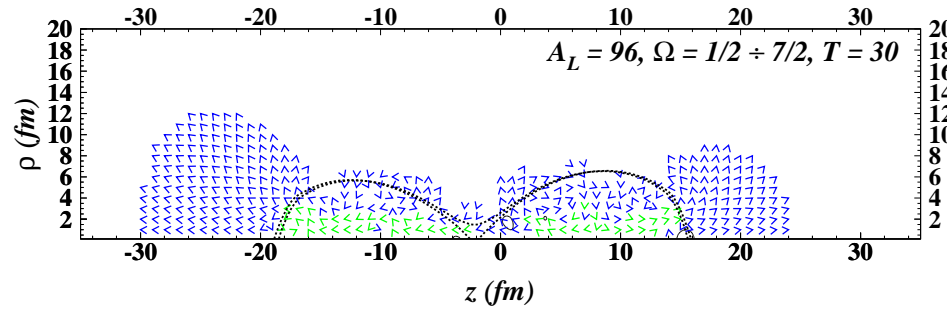
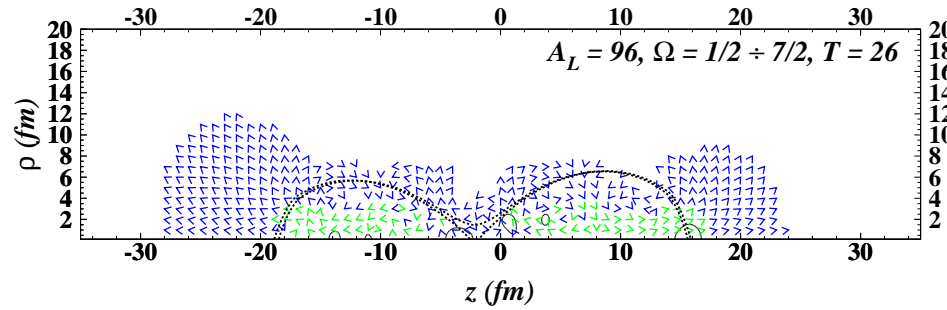
Emission directions ($A_L=96$; all Ω ; $T=14,18,22 \times 10^{-22}$ sec)

emission along the fission axis; the light-fragment is more productive

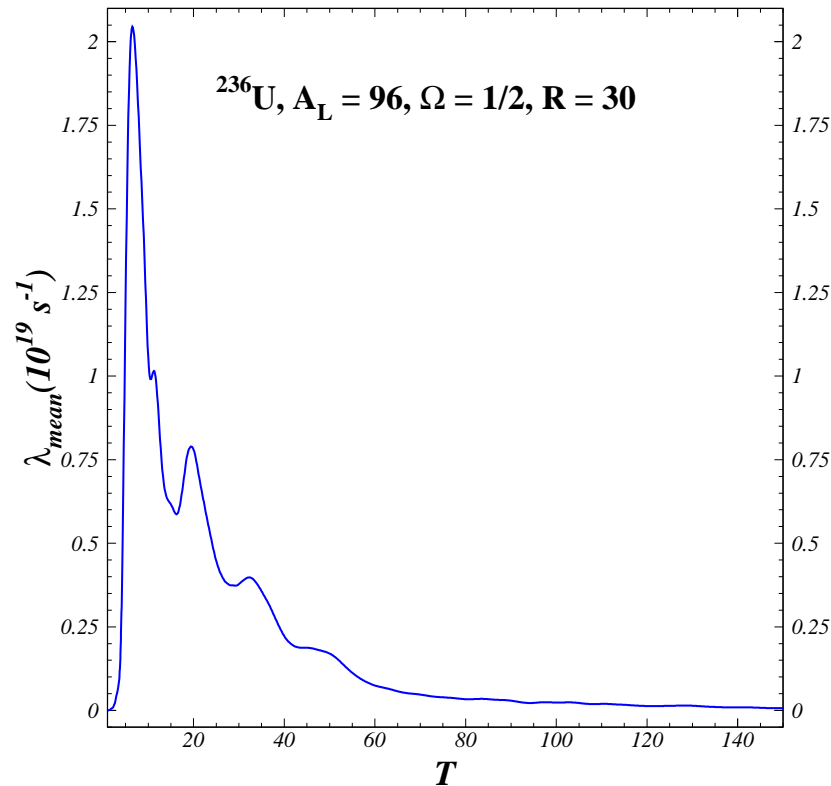


Emission directions ($A_L=96$; all Ω ; $T=26,30,36 \times 10^{-22}$ sec)

emission is slowed down; neutron transfer & reflections



Scission-neutron time-dependent decay-rate



On notices oscillations that reflect a pulsed-emission. Most neutrons are emitted between 5 and $10 \times 10^{-22} \text{ s}$ after scission. For $T > 6 \times 10^{-21} \text{ s}$ the decay rate is almost constant \rightarrow tunnelling from a quasistationary state.

Angular distribution - computational procedure

The core of the [dynamical scission model](#) is the calculation of the time evolution of the neutron states in a nucleus that undergoes scission using the [TDSE](#): [N. Carjan, M. Rizea, Int. J. Mod. Phys. E21 \(2012\) 0031125](#)

To estimate the angular distribution with respect to the fission axis of the neutrons emitted during scission we separate this calculation in two stages:

- 1) The [scission process](#) itself, i.e., the neck rupture and its absorption by the fragments. The nuclear configurations involved are defined by a set of deformations $\{\alpha_i\}$ (when the neck starts to break) and $\{\alpha_f\}$ (when the neck stubs are completely absorbed by the fragments). The duration of this stage is relatively short (e.g. $T = 10^{-22}$ sec) and the potential in which the neutrons move changes rapidly.

Angular distribution - procedure

2) The **detachment** from the fragments of the fraction of the **neutrons that are left unbound** at the end of the previous stage. Since their motion is much faster than that of the just separated fragments, one can, in a first approximation, freeze the fragments at the configuration $\{\alpha_f\}$. Hence the potential in which the neutrons move is kept constant during this stage. We follow the motion of the wave packet that describes the unbound neutrons for as long as we can (4×10^{-21} sec) and calculate the current density at each time step. To obtain the angular distribution one separates the tangential from the radial components of the current along the surface of a large sphere and integrate in time.

Angular distribution - formula

- **The number of neutrons** that leave a sphere of radius R (around the fissioning nucleus) in a solid angle $d\Omega$ and in a time interval dt is:

$$d\nu_{sc}^{em} = \bar{J}_{em}(R, \theta, t) \bar{n}(R, \theta, t) R^2 dt d\Omega.$$

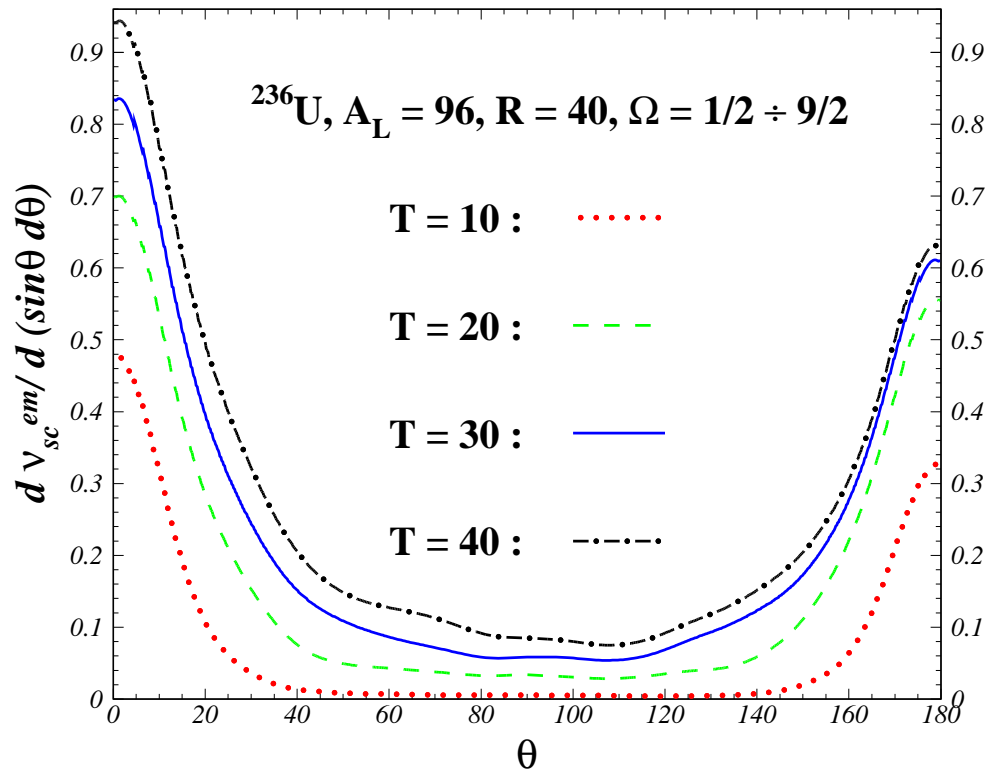
- **The angular distribution** is given by the integral with respect to t of the above quantity. The upper limit should in principle be ∞ . In practice we can reach only a finite value t_{max} .

- **The total number of emitted neutrons** ν_{sc}^{em} at t_{max} is obtained by a further integration with respect to θ ($d\Omega = \sin\theta d\theta$).

A factor of 4π also appears due to the integration over the angle ϕ and to the spin degeneracy.

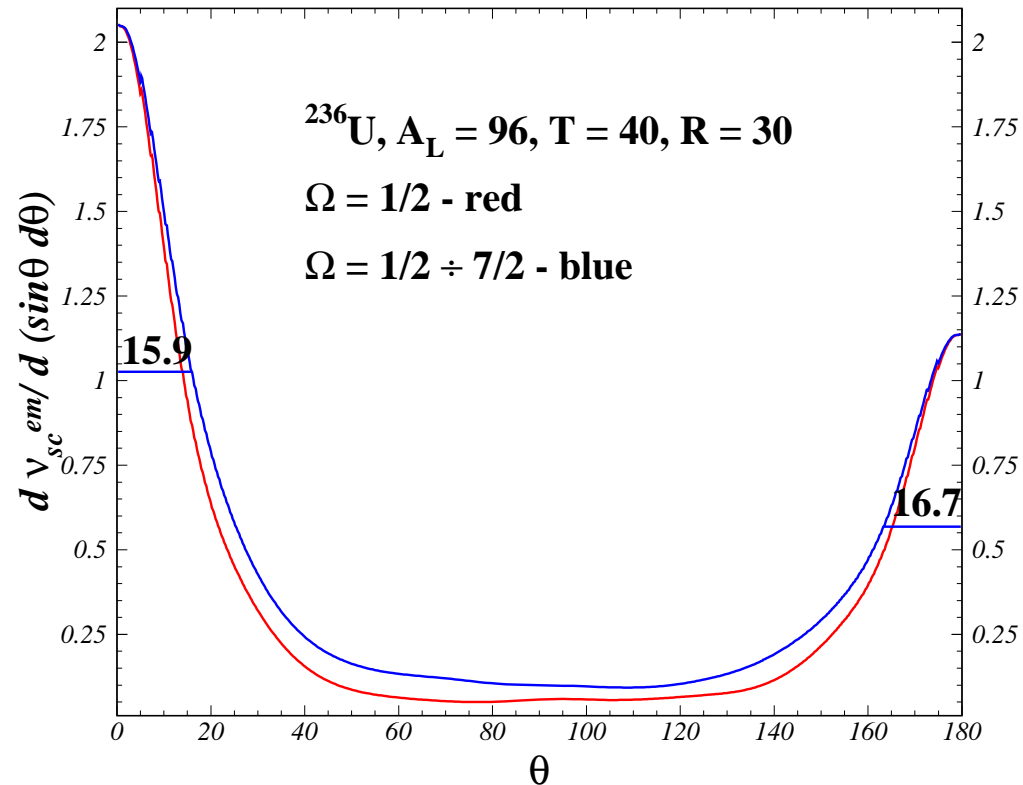
The time evolution of the ang distr for $A_L = 96$ at $R=40$ fm

L and H widths increase with increasing time T by $\approx 3^\circ$.



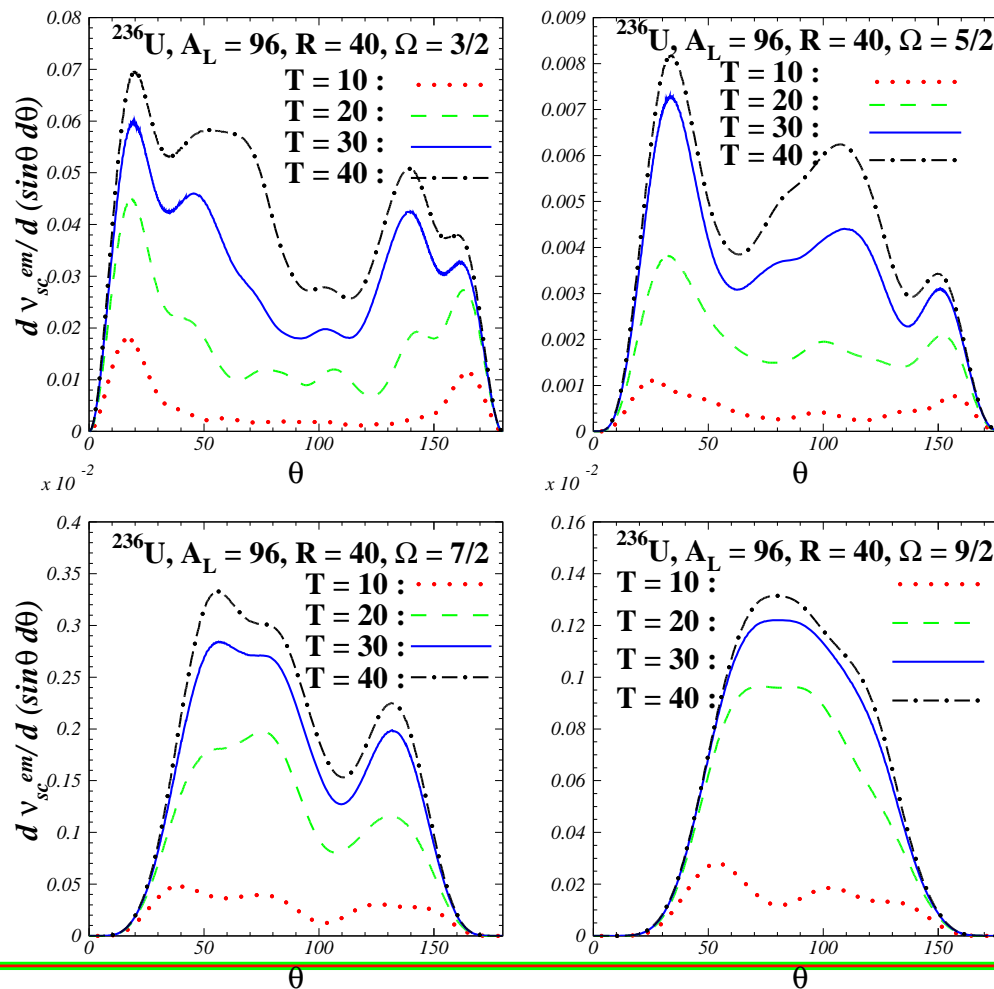
Contribution of $\Omega=1/2$ to the angular distribution

around 0° and 180° there are only neutrons with $\Omega = 1/2$!



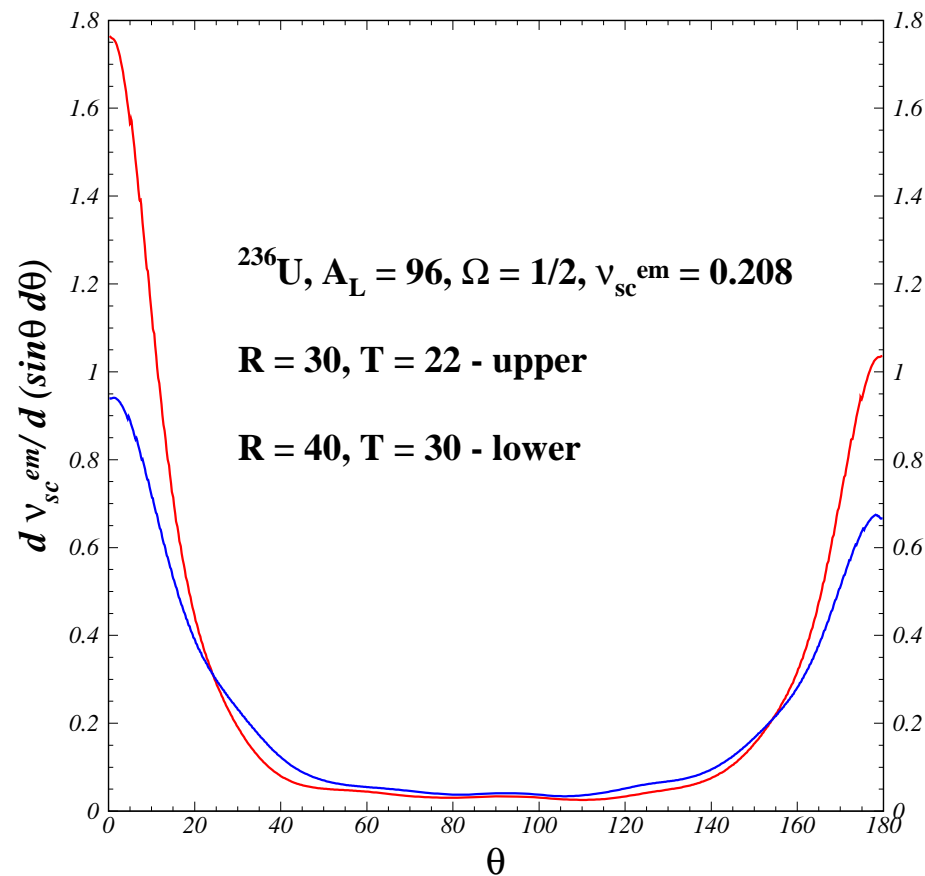
Angular distribution for $\Omega = 3/2, 5/2, 7/2$ and $9/2$

neutrons with high Ω are not emitted along the fission axis

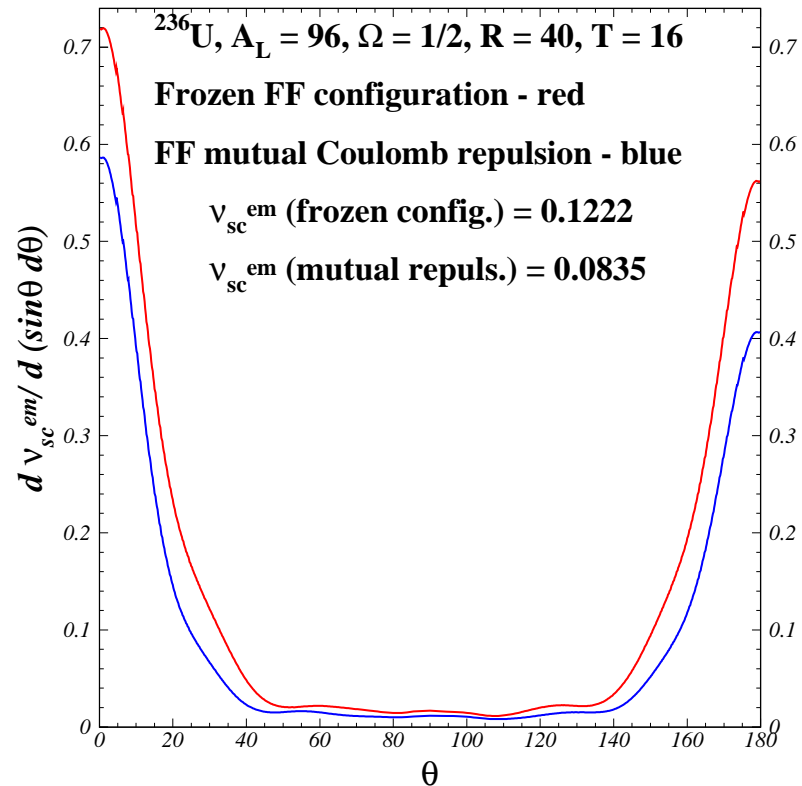


Comparison of the ang distr for $A_L = 96$ at $R=30$ and 40 fm

L and H widths increase with increasing radius R by $\approx 3^\circ$;
convergence is probably not yet attained



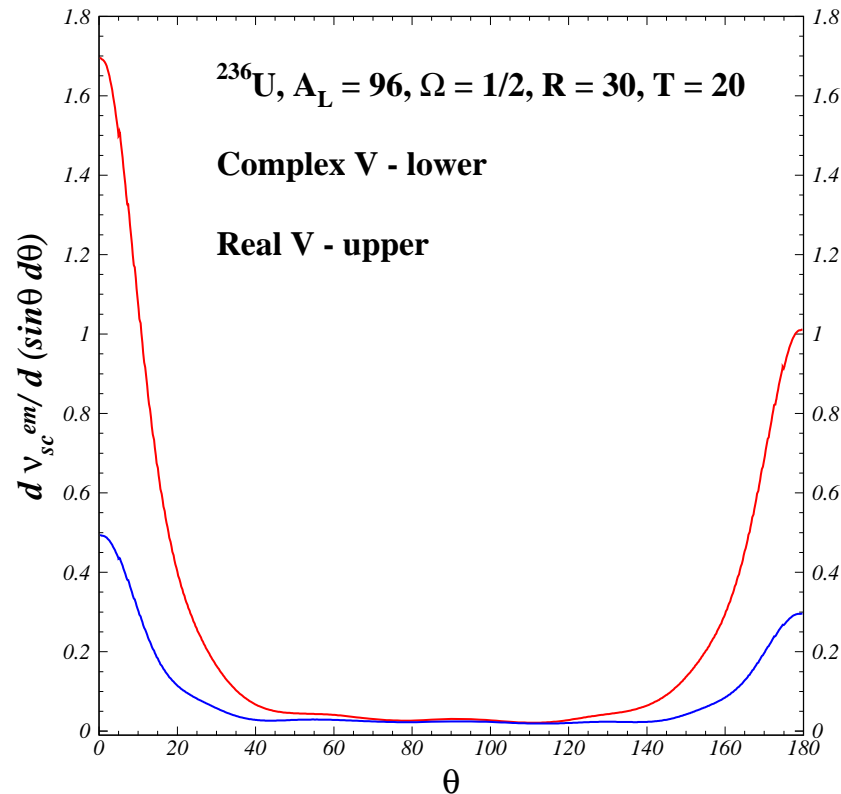
Simultaneous motion of the fission fragments



It slows down the neutron emission!?

It doesn't affect the width.

Role of the imaginary potential ($W_0 = 2MeV$)



As expected: it reduces the scission neutron multiplicity.
Surprisingly: it does not increase the widths of the angular distribution.

Experimental angular resolution

To compare with the experimental data one has to fold with the angular resolution function:

$$\left. \frac{d\sigma}{d\theta} \right|_{\theta=\theta_0} = \int_{-\infty}^{\infty} \frac{d\sigma}{d\theta} r(\theta, \theta_0) d\theta$$

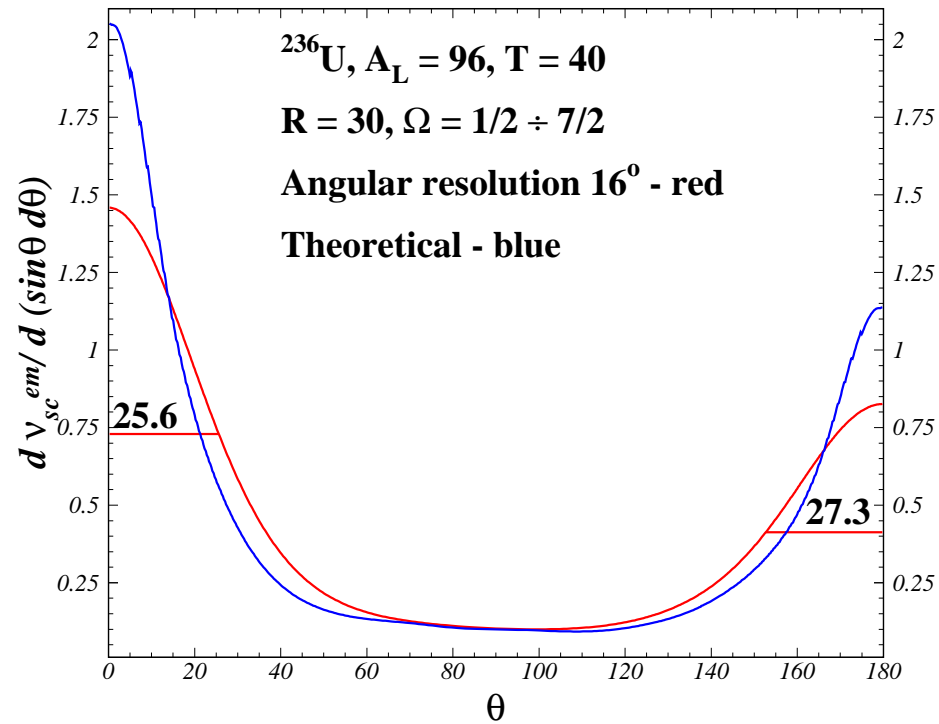
where

$$r(\theta, \theta_0) = \frac{1}{\sqrt{2\pi}\epsilon} \exp \left[-\frac{(\theta - \theta_0)^2}{2\epsilon^2} \right]$$

and $\frac{d\sigma}{d\theta}$ is the angular distribution. The value of ϵ is obtained via the half width:

$$\epsilon\sqrt{2\ln 2} = \Delta\theta_{1/2}.$$

Convolution with the angular resolution function



Remarks on angular distribution

The **angular distribution** of the neutrons emitted at scission is **calculated** starting **with initial conditions given by a realistic scission model** that is dynamical, microscopic and quantum mechanical. It uses nuclear configurations at scission that are appropriate for the main fission mode in the $^{235}\text{U}(n_{th}, f)$ reaction. Although the neutrons are mainly released in the interfragment region, they do not move perpendicular to the fission axis but are drained into the fragments (more into the light one) and finally leave the fissioning system through its tips. They therefore move along the fission axis with an average velocity not too far from the velocity of the fully accelerated fragments. Curiously enough, the ratio ν_L/ν_H is close to the experimental value (1.41) averaged over all fragment pairs.

Remarks on energy distribution

The calculated distribution of the average energies of each neutron released at scission agrees well with the slope and the range of the measured prompt-neutron spectrum.

Conclusions

Unusual process : simultaneous partial emission of all neutrons present in a fissioning nucleus at scission.

Unusual approach: time-dependent shell-model.

Unexpected agreement: with measured properties of prompt fission-neutrons.

⇒ **It is a viable alternative to the evaporation hypothesis.**

Limitations: due to the complexity of the calculations we were not so far able to:

- 1) Use a larger numerical grid than: $\rho_{max} = z_{max} = 42 fm$; but TBC were implemented at the numerical boundary.
- 2) Propagate the wave packet of the unbound neutrons longer than: $4 \times 10^{-21} s$; however the majority of neutrons have left the sphere by then.